

Long distance non-line-of-sight (NLOS) visible light signal detection based on rolling-shutter-patterning of mobile-phone camera

WEI-CHUNG WANG,¹ CHI-WAI CHOW,^{1,*} LIANG-YU WEI,¹ YANG LIU,² AND CHIEN-HUNG YEH³

¹Department of Photonics and Institute of Electro-Optical Engineering, National Chiao Tung University, Hsinchu 30010, Taiwan

²Philips Electronics Ltd., N.T., Hong Kong, China

³Department of Photonics, Feng Chia University, Seatwen, Taichung 40724, Taiwan

*cwchow@faculty.nctu.edu.tw

Abstract: We propose and demonstrate a long distance non-line-of-sight (NLOS) visible light signal detection based on the rolling shutter patterning using commercial mobile phone camera. By using our improved rolling shutter pattern demodulation algorithm, such as the background compensation (BC) blooming mitigation, extinction-ratio (ER) enhancement and Bradley adaptive thresholding, a 1.5 m NLOS visible signal (at low illumination of 145 lux) can be retrieved.

© 2017 Optical Society of America

OCIS codes: (230.3670) Light-emitting diodes; (060.4510) Optical communications; (060.4080) Modulation.

References and links

1. J. R. D. Retamal, H. M. Oubei, B. Janjua, Y. C. Chi, H. Y. Wang, C. T. Tsai, T. K. Ng, D. H. Hsieh, H. C. Kuo, M. S. Alouini, J. H. He, G. R. Lin, and B. S. Ooi, "4-Gbit/s visible light communication link based on 16-QAM OFDM transmission over remote phosphor-film converted white light by using blue laser diode," *Opt. Express* **23**(26), 33656–33666 (2015).
2. H. H. Lu, Y. P. Lin, P. Y. Wu, C. Y. Chen, M. C. Chen, and T. W. Jhang, "A multiple-input-multiple-output visible light communication system based on VCSELs and spatial light modulators," *Opt. Express* **22**(3), 3468–3474 (2014).
3. C. H. Chang, C. Y. Li, H. H. Lu, C. Y. Lin, J. H. Chen, Z. W. Wan, and C. J. Cheng, "A 100-Gb/s multiple-input multiple-output visible laser light communication system," *J. Lightwave Technol.* **32**(24), 4723–4729 (2014).
4. Z. Wang, C. Yu, W. D. Zhong, J. Chen, and W. Chen, "Performance of a novel LED lamp arrangement to reduce SNR fluctuation for multi-user visible light communication systems," *Opt. Express* **20**(4), 4564–4573 (2012).
5. C. H. Kwok, R. V. Penty, and I. H. White, "Link reliability improvement for optical wireless communication systems with temporal-domain diversity reception," *IEEE Photonics Technol. Lett.* **20**(9), 700–702 (2008).
6. C. W. Chow, C. H. Yeh, Y. Liu, and Y. F. Liu, "Digital signal processing for light emitting diode based visible light communication," *IEEE Photon. Soc. Newslett.* **26**, 9–13 (2012).
7. C. W. Hsu, C. W. Chow, I. C. Lu, Y. L. Liu, C. H. Yeh, and Y. Liu, "High speed imaging 3×3 MIMO phosphor white-light LED based visible light communication system," *IEEE Photonics J.* **8**(6), 7907406 (2016).
8. S. Wu, H. Wang, and C. H. Youn, "Visible light communications for 5G wireless networking systems: from fixed to mobile communications," *IEEE Netw.* **28**(6), 41–45 (2014).
9. P. Luo, M. Zhang, Z. Ghassemlooy, H. L. Minh, H. M. Tsai, X. Tang, L. C. Png, and D. Han, "Experimental demonstration of RGB LED-based optical camera communications," *IEEE Photonics J.* **7**, 7904242 (2015).
10. C. Danakis, M. Afgani, G. Povey, I. Underwood, and H. Haas, "Using a CMOS camera sensor for visible light communication," in *Proc. OWC'12* (2012), pp. 1244–1248.
11. C. W. Chow, C. Y. Chen, and S. H. Chen, "Enhancement of signal performance in LED visible light communications using mobile phone camera," *IEEE Photonics J.* **7**(5), 7903607 (2015).
12. K. Liang, C. W. Chow, and Y. Liu, "Mobile-phone based visible light communication using region-grow light source tracking for unstable light source," *Opt. Express* **24**(15), 17505–17510 (2016).
13. D. Bradley and G. Roth, "Adaptive thresholding using the integral image," *J. Graph. GPU Game Tools* **12**(2), 13–21 (2007).
14. ISO/IEC 18004:2000. Information technology-Automatic identification and data capture techniques - bar code symbology - QR Code (2000).

1. Introduction

Wireless communications using optical frequencies to carry information (known as optical wireless communication (OWC)) has regained attentions recently [1–5]. The continuous improvement of efficiency and reduction in cost of white light emitting diode (LED) allow it to be widely deployed in lightings. Using the white light LED for lighting and communication in visible light communication (VLC) has attracted many attentions nowadays [6]. Gigabit-per-second VLC transmission using white light LED has been demonstrated [7]; and it could be a promising technology for the next generation 5G mobile communication system [8].

As the mobile phones with embedded complementary-metal-oxide-semiconductor (CMOS) camera become common, using these cameras as VLC receivers (Rxs) can significantly reduce the cost of VLC deployment and increase the user flexibility. However, the commercially available camera has a limited frame rate (frame per second, fps) of only 30/60 fps. When the camera is deployed for the VLC detection, a data rate of only 150 bit/s (3 x 50 bit/s when using red-green-blue LEDs) is achieved [9]. By using the rolling shutter effect of the CMOS camera, the detection data rate can be significantly enhanced [10–12]. By deploying different techniques, such as blooming mitigation and extinction ratio (ER) enhancement, the demodulation and the synchronization of the received rolling shutter pattern can be greatly improved, and a net data rate of 5.76 kbit/s was reported recently [12].

In this work, we propose and demonstrate a long-distance non-line-of-sight (NLOS) visible light signal detection using commercial mobile phone camera. By using our improved rolling shutter pattern demodulation algorithm, such as the background compensation (BC) blooming mitigation, extinction-ratio (ER) enhancement and Bradley adaptive thresholding; and together with using higher International Standards Organization (ISO) camera sensitivity and shorter shutter speed setting, a 1.5 m NLOS visible signal can be received and demodulated; and carrying 96 bits (12 ASCII characters). The illumination of only 145 lux is needed. Signal performances and the processing times are evaluated.

2. Experiment and algorithm

Figure 1 illustrates the scenarios of using white LED for lighting and VLC simultaneously. Fig. 1(a) and 1(b) represent the LED light is on and off respectively. As the LED is modulated at the frequency higher than the response of human eye, we cannot experience light flashing. If the VLC Rx has high enough sensitivity, the NLOS visible light signal detection is feasible even though the Rx is not directly pointed towards the LED light. By using the rolling shutter effect of the CMOS camera, the exposure of all pixels is not performed at the same time; but instead, the pixel row in the camera is activated sequentially. Hence, bright and dark fringes will be captured in an image frame when LED light is on and off respectively. By using our improved rolling shutter pattern demodulation algorithm and using higher ISO camera sensitivity setting (in manual mode), much lower illumination and longer detection distance can be achieved. In the experiment, we adjust the exposure time as small as possible (125 μ s) to avoid the inter-symbol interference (ISI), and adjust the ISO as large as possible (1600) to increase the Rx sensitivity.

Figure 2 shows the experimental setup of the NLOS VLC system using CMOS camera. The VLC data is constructed using Matlab®, and it is applied to two phosphor-based white-light LED chips (Cree® XR-E) with color temperature of 5500 K via an arbitrary waveform generator (AWG, Tektronix® AFG3252C) with sampling rate of 2 GSample/s and bandwidth of 240 MHz. The mobile phone (HTC® A9) has the CMOS camera with resolution of 2367 x 4208 pixels. The exposure time and the ISO settings in manual mode are 1/8000 s and 1600 respectively. In the proof-of-concept experiment, a piece of white A4 paper is used to emulate the wall for NLOS detection, and the visible signal synchronization and demodulation is performed by using offline Matlab® program. It is worth to note that they can also be performed using the application program of the mobile phone. On-off keying (OOK) modulation format is used in each VLC packet, which consists of a 12-bit header for

synchronization and a 96-bit to 172-bit payload. Each VLC packet is transmitted twice sequentially. Figure 2 also illustrates that during the NLOS demonstration, the distance between the LEDs and the paper (d_1) will increase from 50 cm to 200 cm, and the distance between the paper and the mobile phone (d_2) is fixed at 15 cm.

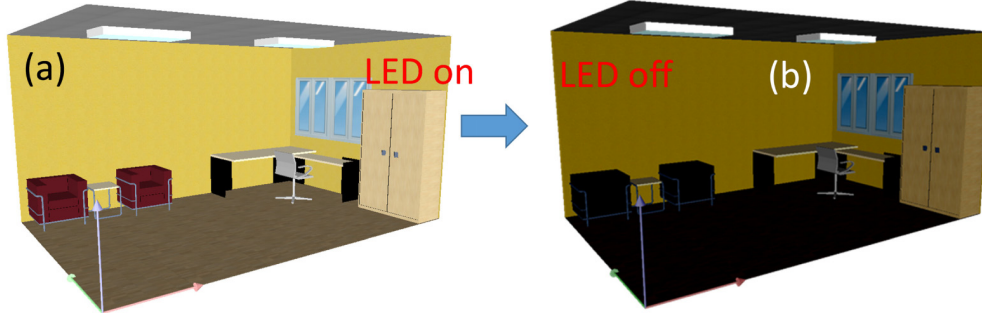


Fig. 1. Scenarios when the LED is (a) on and (b) off.

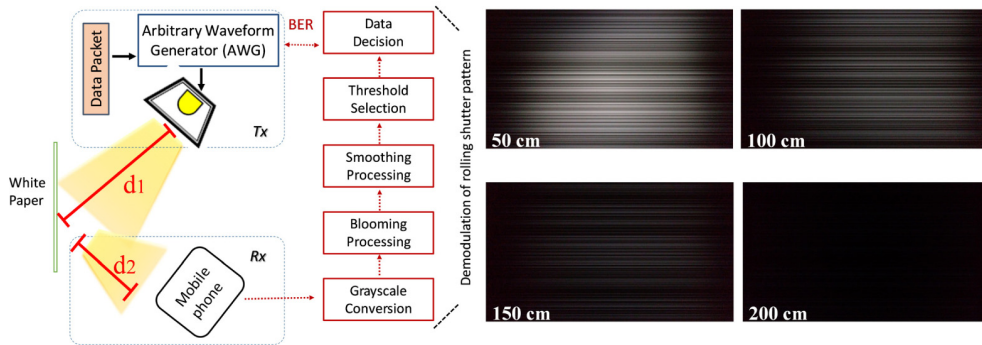


Fig. 2. Experimental setup of the NLOS VLC system using CMOS camera to capture the visible signal. Insets: Experimental image frames captured by the CMOS camera in different NLOS conditions.

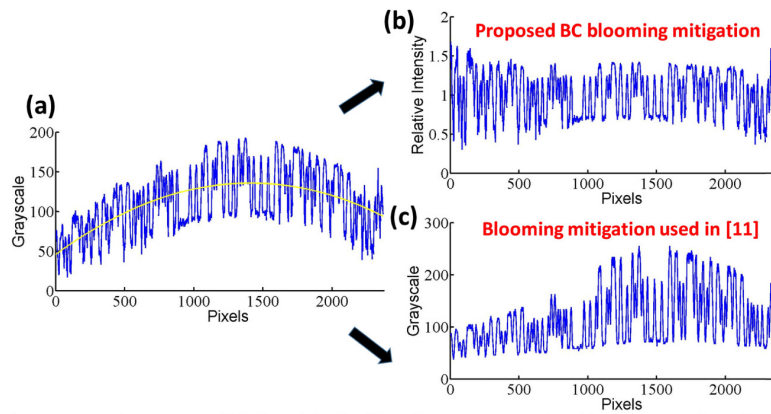


Fig. 3. Grayscale patterns of (a) the original rolling shutter pattern, after (b) the proposed BC blooming mitigation, and (c) the blooming mitigation used in [11].

Insets of Fig. 2 show the experimental image frames captured by the CMOS camera in different NLOS conditions. Bright and dark can be observed. Although the fringes are hardly to be seen when the distance between the LEDs and the paper is 200 m (i.e. the total optical path between the LEDs and the camera is 215 cm), after the demodulation by our proposed scheme, the data can be managed to retrieve. In the rolling shutter pattern demodulation, the

first step is to convert the color rolling shutter pattern into grayscale pattern. Figure 3(a) shows the grayscale pattern (0 – 255) obtained from the rolling shutter pattern. The pixels in the image center are saturated (i.e. higher grayscale values) by the blooming effect. Then, our developed BC blooming mitigation algorithm is applied, and the final grayscale pattern is shown in Fig. 3(b). In the BC blooming mitigation, a second order polynomial fitting of the grayscale values of the original grayscale pattern is obtained, as illustrated by the yellow curve in Fig. 3(a). This yellow curve also represents the distribution of light intensity at the grayscale column we chose. Then the yellow curve values is divided by the original grayscale pattern, and the blooming mitigated grayscale pattern as shown in Fig. 3(b) is obtained. We also compare with other blooming mitigation algorithm described in [11] as shown in Fig. 3(c). We can see that the grayscale value fluctuation of our proposed BS blooming mitigation scheme is much smaller.

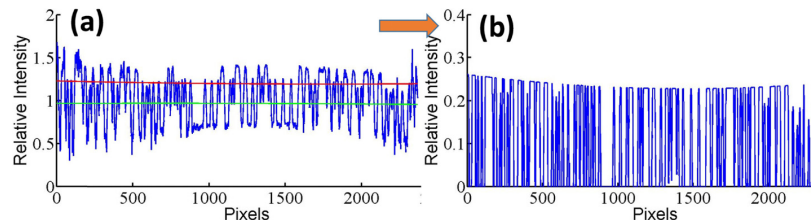


Fig. 4. Grayscale patterns (a) after BC blooming mitigated and (b) after ER enhancement.

Then the ER enhancement scheme is applied. In this scheme, a second order polynomial fitting (the red curve) is constructed to the blooming mitigated grayscale pattern in Fig. 4(a). When the grayscale value is larger than the red curve, it is set equal to the red curve. Then another second order polynomial fitting (the green curve) is constructed in Fig. 4(a). When the grayscale value is smaller than the green curve, it is set equal to the green curve. Hence, the ER enhanced grayscale pattern as shown in Fig. 4(b) can be obtained.

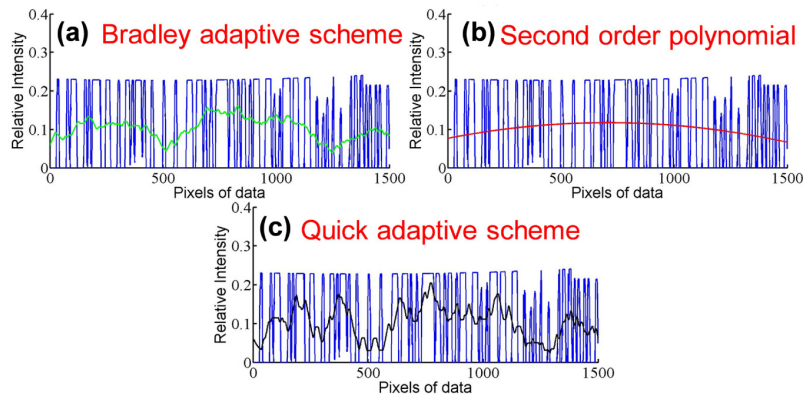


Fig. 5. Experimental grayscale values after (a) Bradley thresholding, (b) second order polynomial thresholding, and (c) quick adaptive thresholding.

Finally, we need to distinguish the data logic, and we apply our proposed modified Bradley adaptive scheme. The Bradley adaptive scheme is usually applied in the image processing to identify image object [13]; here we apply for identifying the data logic in the rolling shutter pattern. This scheme is to divide the whole grayscale pattern into different sections and calculate the average grayscale of each section. The Bradley adaptive thresholding scheme, like other thresholding schemes, is to define the threshold values for the changing data patterns; hence the logic 1 or logic 0 can be identified. During the Bradley adaptive thresholding, every 60 pixels are selected as a group (i.e. $s = 60$). Let y_i be the grayscale value of a pixel at point i , and the threshold T_i will be the average grayscale value of the sum of the range with y_i as the center. Hence, the threshold can be obtained in Eq. (1).

$$T_i = \frac{1}{S} \sum_{n=-s/2}^{s/2} y_{i+n} \quad (1)$$

As Bradley thresholding is an adaptive scheme, it can perform much better when compared with the polynomial fitting thresholding scheme [12] (not adaptive) in manipulating the fast changing data patterns. As the Bradley thresholding performs the average grayscale value in a group, while the quick adaptive thresholding [12] performs the weighted average grayscale value in a group; the Bradley thresholding scheme can be more efficient. Besides, the proposed Bradley adaptive thresholding scheme, we also compare several thresholding schemes reported in the literatures [11, 12]. Figures 5(a)-5(c) show the grayscale values after different thresholding schemes are applied. The green, red and black curves represent the proposed Bradley thresholding, second order polynomial thresholding, and quick adaptive thresholding respectively. It is worth to mention that the data pattern shown here is from only one image frame. In random image frames captured by a mobile phone camera, because of the light intensity and focus position are not fixed; proper thresholding schemes are required for data logic identification.

3. Results and discussions

The bit-error-ratio (BER) performances are evaluated and compared based on the three thresholding schemes as discussed in Fig. 5 using the same visible signal obtained from the CMOS camera. The BER performance evaluation is based on the actual error counting by comparing the received data and the original transmitted data. For example, when there are 2 error counts when transmitting the 172-bit data, the $BER = 2/172 = 0.0116$. The illumination (a measure of how much luminous flux spread over a given area) measured by a lux-meter is also included in Fig. 6. Here, two kinds of payload (96-bit and 172-bit) are under evaluation, while the header is 12-bit. The distance d_l are 50 cm, 100 cm, 150 cm and 200 cm, and the corresponding illuminances are 430 lux, 250 lux, 145 lux and 65 lux respectively. As shown in Fig. 6, since the second order polynomial thresholding is not accurate enough for the fast changing data, at low luminance, highest BER is observed among the three schemes. On the other hand, at the transmission distance d_l of 150 cm, where the illumination is 145 lux, we can observe that the proposed Bradley thresholding performs as well as the quick adaptive thresholding scheme when the visible signal is carrying 96 bits payload data, and no error count is measured for both schemes. As reported in [12], the quick adaptive thresholding is to calculate a moving average of grayscale values of pixels, it is much more complicated than the Bradley thresholding scheme in which the Bradley scheme only uses the averages of different sections. When the transmission distance is further increased to 200 cm, where the illumination is only 65 lux, we can observe that the Bradley adaptive thresholding has a higher error count than the quick adaptive scheme.

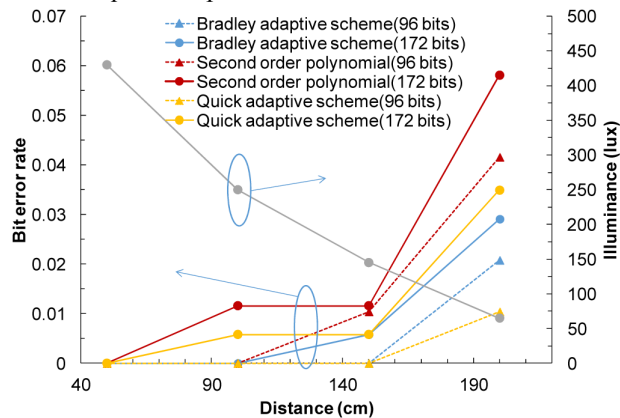


Fig. 6. Measured BER performances and the illuminance at different transmission distances.

Figure 7 shows the measured net data per frame at different transmission distances. In this evaluation, Bradley adaptive thresholding scheme is applied and no error count is allowed at the Rx. We can observe that even at 200 cm transmission distance, 68 bit per frame can be achieved with error free. The processing times of different thresholding schemes and the ratios to the minimum processing time are shown in Table 1. It is obvious that the second order polynomial threshold is the fastest, but with higher error counts. It is worth to note that although the quick adaptive scheme has outstanding performance, it needs much more time than Bradley adaptive scheme. When comparing the proposed rolling shutter patterning scheme with the popular quick response (QR) coding scheme [14], we can see that both schemes can work well with commercial available mobile phone camera. And the QR coding can support much more information, for example, in the version 1 of 21 x 21 modules, 152 bits can be transmitted by using the low level of error correction code (ECC). Some higher density QR code can carry thousands of bits. However, our proposed rolling shutter patterning scheme can support long distance (> 1.5 m) and NLOS detection. Besides, the information content can be updated flexibly, while the QR code information is usually fixed.

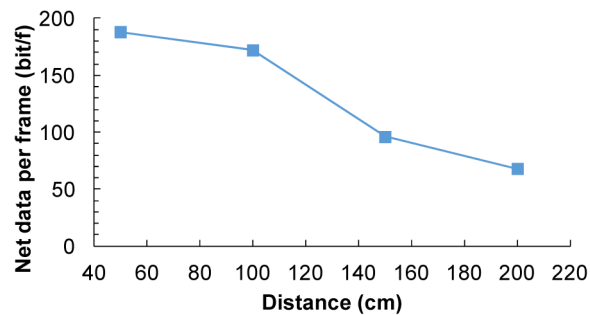


Fig. 7. Measured net data per frame at different transmission distances.

Table 1. Processing time of the three thresholding schemes and their relative time required.

		Time(second)	Ratio
Second Order	96 bits	0.00158	1
Polynomial	172 bits	0.00279	1.011
Bradley	96 bits	0.00189	1.196
Adaptive	172 bits	0.00276	1
Quick	96 bits	0.01243	7.867
Adaptive	172 bits	0.01278	4.63

4. Summary

We proposed and demonstrated for a long-distance NLOS visible light signal detection using commercial mobile phone camera. By using our improved rolling shutter pattern demodulation algorithm, such as the BC blooming mitigation, ER enhancement and Bradley adaptive thresholding, a 1.5 m NLOS visible signal (at low illumination of 145 lux) can be retrieved without any error count.

Acknowledgments

This work was supported by Ministry of Science and Technology, Taiwan, MOST-104-2628-E-009-011-MY3, Aim for the Top University Plan, Taiwan, and Ministry of Education, Taiwan.